ICAS 96

Sorrento, Italy

Guggenheim Lecture

Smart Structures in Aerospace Technology

Paolo Santini

Dipartimento Aerospaziale, Università di Roma "La Sapienza"

Work performed with the support of University of Rome "La Sapienza" and

Ministero della Ricerca Scientifica e Tecnologica

May 1996

Abstract

Smart components are more and more widely used in Aerospace structures, since they offer new possibilities for distributed control. Of the several kinds of smart sensors and actuators, only piezo components are considered in the paper. General methods of solution are described with reference to very simple examples, such as beams and plates, in order to outline main features and problems with this kind of control. In particular, the well known problem of structure-piezo interaction is discussed.

Another problem of interest is the adequacy of stiffening and damping properties, that must be such that application of smart component will really be able to improve structural characteristics. Mathematical conditions for this to happen are very briefly discussed.

As for fields of real interest in Aerospace Technology, torsion and associated aeroelastic properties could in principle receive some substantial help from Smart Structures, but available robustness and authority are not yet sufficient. Also, wave propagation control is discussed, essentially on simple schemes: the idea is substantially to have active regions where wave amplitudes are measured, and actuators are placed in such a way as to have closed loop dispersion functions capable of suppressing some unwanted vibrations outside the active region. Analytical formulations, numerical examples and bibliography complete the work.

It should be noted that this manuscript is delivered to ICAS around May 20th 1996. Since the final presentation is scheduled for September, it is likely that new material will be added.

1 Introduction

Receiving the Guggenheim Award is a great honour for an aeronautical engineer, or researcher. It is surely one of the highest acknowledgments in the world, a distinction everyone operating in our field can desire after a long career, as it is in my case. But the recipient has some rules to respect. First of all, to write a paper on a subject he can choose, and, I have been requested, the paper should not be a review of what has been done and of what is being done in the field that has been indicated by the Author.

For the rest, I have been left, and I felt, free to tune my writing and my presentation according to my views and my style.

People like me have the task to understand things and to help other, probably more active, people, to understand those things. So, I tried to expound what seemed to me to be the basic ideas of the research and exploration in the field of Smart Structures in the aerospace

domain. This is the field to which today, probably, the highest density of scientific meetings is corresponding, since it has its roots in the modern mentality of controls: whatever event, not only in the technical field, should be controlled, leaving nothing outside the human will, or, even worse, leaving it to hazard. It should be borne in mind that a Guggenheim lecture is not a lecture for specialists only, but for the common public.

There are several kinds of applications of smart structures technology. The general idea is, obviously to aid to improve performances of an aerospace machine, avoiding unpleasant phenomena such as excessive, or at least uncontrolled, movements and deformations, reducing overall, or local, stability.

This is especially achieved through a proper increase of structural rigidity and/or a proper enhancing of structural damping.

Other applications would refer to Health and Usage Monitoring Systems (HUMS), which is not treated here, but is a very promising field, since it tries to answer a question everybody has: how long is this piece of machinery going to live? My personal view is that, in some decades, HUMS could be applied to human body too, although I am not sure I would be happy to use it.

Smart Structures Technology, as such and as an independent discipline, started some 20-25 years ago, and just now it starts showing cost benefits. Many important papers [1][2][3] have shown how distributed sensors and actuators have opened the opportunity to apply distributed control to problems where concentrated controls through electric or hydraulic actuators seemed too heavy, not sufficiently reliable or efficient.

The physical principles on which smart components are based are well known: piezoelectricity, shape memory (for some alloys), magnetostriction, electrostriction, and so on. Probably the most popular are piezoelectric actuators and sensors, to which this lecture is devoted, also because it is the field in which I am currently and deeply involved with my School of enthusiastic, wonderful young engineers.

The great problem with piezo components is that their authority as controllers is not yet sufficient for the aims of modern technology. Piezoelectric coefficients are very small (see App.X), and the maximum sustainable electric field should not exceed some $1000 \ V/mm$, and also this limit should be considered in the general field of overall onboard safety in aerospace applications. So the maximum attainable free-strain, which is a real index of the control authority, is of the order of magnitude of 300-$400\mu\varepsilon$.

This has led somebody to say that Smart Structures have been probably oversold [4], also because transition from laboratory environment to real environment has proven to be more difficult than expected. So smart control is really efficient or simply viable only for those problems where amplitudes to be controlled are reasonably small. Prime candidates are in the acoustic field (panel acoustic fatigue is a typical example), although here another problem may arise from high modal density. It seems for the moment rather difficult to efficiently control problems where forces are great (such as, for instance, divergence), also because many of such problems are associated with torsional facts, in which smart components are not very efficients, as we will see.

In my opinion, this is a field in which a close collaboration between technologists and engineers is mostly desirable. Is it possible to "design" a material with some specific characteristics? New modern ideas, such as virtual manufacturing, smart production (which does not mean production of smart materials) could help a lot in this area, providing the community with what everybody is waiting for, i.e., higher authority components.

But further improvements are needed also as far as durability, which has not yet been proved, is concerned. It is of smart sensors and actuators what has been of composites which were seen rather suspiciously some thirty years ago and are now being used more and more widely. The list of aerospace engineering problems in which smart structures have been used or are considered for use is rather lengthy, and it is reported in Appendix VIII: each of them would deserve a discussion, a proper analysis, a bibliography index, etc. Unfortunately (or, better, fortunately for me), this is outside the scope of this paper. I would also like to mention another technique to which, in my opinion, not sufficient attention has been devoted, and it is the active control of wave propagation in a

XXX

one-dimensional continuum, that can be considered as a waveguide where disturbances propagate and are reflected and transmitted. One can think to control structural vibrations by altering the properties of transmissions of some elements in such a way as to prevent them to be transmitted to all the structure, or at least to a critical region of interest. Some criticism was made to this idea on the basis that is applies only to one-dimensional problems: forgetting however, or possibly not knowing, that a wing or fuselage structure, whose interest in aerospace is out of question, is a one dimensional finite continuum, perhaps with some thousands of degrees of freedom, but one-dimensional. We will see it.

2 A general formulation

The equilibrium equation for a continuous body $\mathcal{B}$ reads

$$\left\{ \begin{array}{lll} \nabla\sigma - p & = & 0 \quad \text{in } \mathcal{B} \\ R\sigma - q & = & 0 \quad \text{on } \partial\mathcal{B} \end{array} \right. \qquad (1)$$

The meaning of the symbols is explained in Appendix I. The constitutive equations for a piezoelectric material [5] are written:

$$\left\{ \begin{array}{lll} \varepsilon & = & S^E\sigma + \mathsf{d}E \\ D & = & \mathsf{d}^T\sigma + P^\sigma E \end{array} \right. \qquad (2)$$

Again, for symbols, see Appendix I.
Solving the first of eqs.(2) for σ and substituting into eqs.(1) yields:

$$\left\{ \begin{array}{lll} \nabla(H\varepsilon) - p & = & p_E \quad \text{in } \mathcal{B} \\ R(H\varepsilon) - q & = & q_E \quad \text{on } \partial\mathcal{B} \end{array} \right. \qquad (3)$$

where $H = \left[S^E \right]^{-1}$ and:

$$\left\{ \begin{array}{lll} p_E & = & \nabla(H\mathsf{d}E) \\ q_E & = & R(H\mathsf{d}E) \end{array} \right. \qquad (4)$$

The l.h.s. of (3) are the same of the classical theory of elasticity: so p_E, q_E play the same role as p, q; in other words, they can be considered as additional (or piezoelectric) forces. From this point of view, the situation is very similar to the problem of Thermoelasticity, or Thermal Stresses Analysis.
For a complete solution of the problem one should also write the equations ruling the electrical diffusion within the body, coupling it with (3), then solve the partial differential system arising from the coupling, with the relevant boundary and initial condition. This has not been done in the paper, where E (or, better, the electric potential defined by $E = grad\ V$) is supposed to have a known spatial distribution, whereas its time variation is ruled by control purposes. It should also be noted that the coefficients in (4) need not to be constant; in particular, not all the elements are piezoelectric and at the boundary between piezoelectric and non-piezoelectric mutual forces have the same expression as q_E.
It is seen, however, that the electrical field has a driving capacity, or *actuator effect*, generating forces whose value and variation are capable of providing the required control. On the other hand, by eliminating σ between the two eqs. (2), one obtains:

$$D = \mathsf{d}^T H\varepsilon + (P^\sigma - \mathsf{d}^T H\mathsf{d})E \qquad (5)$$

It is clear, from (5), that one can have an electric displacement even if $E = 0$. This means that a piezo element can act as a sensor too, providing electric charges (associated to D) and consequently feedback current and voltage, in order to achieve the requested control.

3 Application to structural dynamics

We consider now the case of thin-walled structures (which are the only ones of interest in aerospace applications) in which (or just on the surface of which) we place piezoelectric patches. A finite element approach is the tool we generally have at our disposal.
Now, if we consider eqs.(3) we see that nothing new arises as far as the l.h.s. terms are concerned, giving rise to mass, stiffness, structural damping matrices and the load vector. We may account for the piezoelectric terms as for an increase in total potential energy, given (for the j-th element) by:

$$\mathcal{U}_j = \int_{\mathcal{B}_j} w^T(x_1, x_2, x_3)\,\nabla(H\mathsf{d}E_j)\,d\mathcal{B}_j +$$

$$+ \int_{\partial B_j} w^T(x_1, x_2, x_3) \, R(H \mathrm{d} E_j) \, d(\partial B_j) \quad (6)$$

where w is the generic displacement vector in B_j. Denoting by X_j the values of the degrees of freedom relevant to B_j we can write

$$U_j = X_j{}^T P_j E_j \quad (7)$$

where we suppose that E_j remains constant within the piezoelectric part of B_j, although it can vary from patch to patch. The expression of matrix P_j is given in Appendix II. So, finally, the dynamical equation of the structure for the degrees of freedom described by the vector X reads (with obvious meaning of the symbols):

$$\mathbf{M}\ddot{X} + \mathbf{H}\dot{X} + \mathbf{K}X = F + \mathbf{P}E \quad (8)$$

where E is the electric field vector, F the external load vector and $\mathbf{P}$ the matrix of P_j's, properly assembled.

4 Illustrative example: a smart beam

We consider the structure of fig.(1); here we have a beam, with N pairs of piezoelectric patches, symmetrically placed along its upper and lower surface. Physical dimensions and positions of patches are assumed to be given, but, for the moment, not specified.
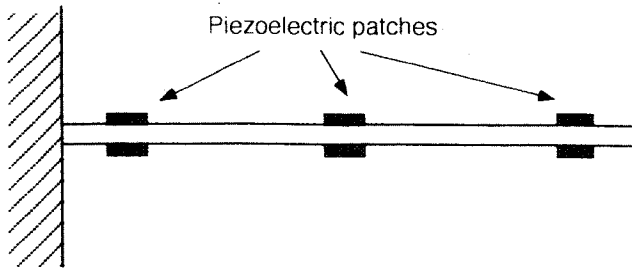
Figure 1: General layout of a smart beam

As we will see, this is a rather simple example, but we can learn much from its analysis, in view of further applications to more complicated and general strucures [6]. We will study two different kinds of connections between patches and hosting structure: the first kind is when the

patch (considered as an extensional bar) is attached to the beam via a rigid member, see fig.(2), and is elsewhere free; the second case, shown in fig.(3), is that of a continuous bondage between patch and beam, which have the same displacements at the interface.
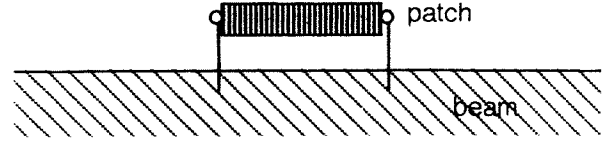

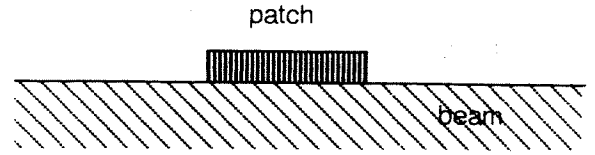Figure 2: Pin-jointed connection

Figure 3: Full-bondage (continuous) connection

Let us start by treating the problem in the frequency domain. We easily find the end-forces on the k-th patch in terms of the (transformed) beam rotations $\bar\theta_0^k$, $\bar\theta_1^k$ at the patch ends. Now, if we apply positive voltage $\bar V_k$ on the upper patch, and equal and opposite voltage on the lower patch, we have control moments given by:

$$\bar M_0^k = c_{00}^k \bar\theta_0^k + c_{01}^k \bar\theta_1^k + \nu_0^k \bar V_k \quad (9)$$

$$\bar M_1^k = c_{10}^k \bar\theta_0^k + c_{11}^k \bar\theta_1^k + \nu_1^k \bar V_k \quad (10)$$

The values of the coefficients c^k and ν^k for the k-th actuator are given in App. III.

If we now introduce the vector $\bar\Theta$ of the nodes rotations, the vector $\bar M$ of the nodal moments, the vector $\bar V$ of the actuator voltages, and we denote by ν and C the properly assembled matrices of ν_j^k and c_j^k, we can write eqs.(9)-(10) as

$$\bar M = C\bar\Theta + \nu \bar V \quad (11)$$

Since the rotations must be the same on the beam and on the patches, the f.e.m. version of the host structure equation reads:

$$\bar\Theta = G_m(\bar M + \bar M_A) + G_f \bar F_A \quad (12)$$

where G_m is the matrix dynamic Green's function that links rotations and bending moments, G_f is Green's function relating rotations with forces, $\bar{M}_A$ and $\bar{F}_A$ are applied moments and forces, if any. From (11) and (12):

$$\bar{\Theta} = Z_A \bar{V} + \bar{\Theta}_A \tag{13}$$

where

$$Z_A = \left(G_m^{-1} - C\right)^{-1} \nu$$
$$\bar{\Theta}_A = \left(I - G_m C\right)^{-1} \left(G_m M_A + G_f F_A\right)$$

Z_A is often referred to as the electromechanical impedance matrix, or open-loop transfer function of the system [7][8].

Consideration of the above scheme may give rise to some criticism, due to the fact that the piezo patch does not fully take part in the host structure motion (in the specific case, the transverse motion of the beam). For this reason, a more realistic scheme to use is that correspondig to an actuator completely bonded to (or imbedded in) the host structure. In this case, we simply ignore the contribution of C in eq.(11), and take for G_m and G_f Green's functions obtained by adding the stiffness and mass of the piezo to the stiffness and mass of the beam.

The beam is now activated, but not yet controlled. For this purpose, we must relate the input $\bar{V}$ to $\bar{\Theta}$ and its time derivatives through amplifier factors g_c^0 and g_c^1:

$$\bar{V} = (g_c^0 + j\omega g_c^1)\bar{\Theta} \tag{14}$$

It shold be noted that g_c^0 and g_c^1 are to be chosen according to the control strategy to be planned. The control system must transform measureable output quantities into input control voltage. For this reason, in reality the measured quantities upon which control is based, are electrical charges and currents on the sensor faces, strictly related to $\bar{\Theta}$ and $d\bar{\Theta}/dt$ (see App.III) [9].

From (14) and (13) we obtain the relation

$$\bar{\Theta} = \bar{Z}_C \bar{\Theta}_A \tag{15}$$

with the closed loop transfer function:

$$\bar{Z}_C = \left[I - Z_A \left(g_c^0 + j\omega g_c^1\right)\right]^{-1} \tag{16}$$

From the knowledge of $\bar{Z}_C$ we can obtain the time domain results, once given the expressions for $M_A(t)$ and

$F_A(t)$.

A better perspective to the problem can be gained using time domain analysis. Here it is convenient to write the equation of motion under the form:

$$a_m \mathbf{M}^* \ddot{X} + a_h \mathbf{H}^* \dot{X} + a_k \mathbf{K}^* X =$$
$$a_c^0 \mathbf{L}^* X + a_c^1 \mathbf{L}^* \dot{X} + F \tag{17}$$

where quantities with an asterisk are nondimensional quantities, F is the external load vector and X are nondimensional degrees of freedom.

The dimensional coefficients a_m, a_h, a_k, a_c^0 and a_c^1 are a measure of the importance of the various terms in the total balance. For the specific case under concern, their value is given in App.III.

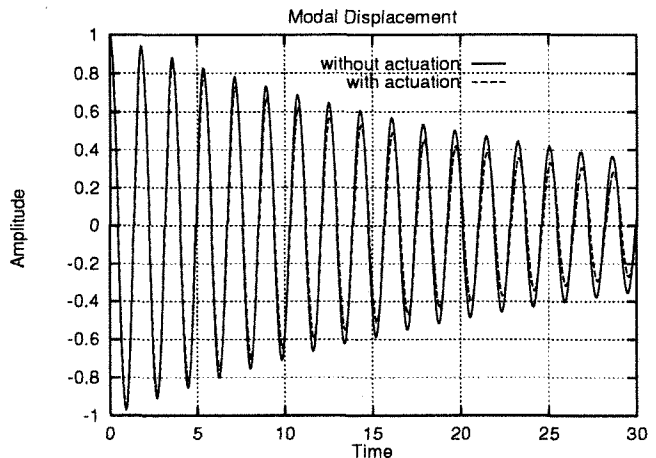| Characteristics	Beam	PZT
Length (mm)	2000	1000
Width (mm)	400	400
Thickness (mm)	40	0.2
Young's Modulus $(N/m^2 \times 10^9)$	70	63
Mass Density (kg/m^3)	2700	7630
PZT constant $(m/volt \times 10^{-9})$	-	180

Table 1: Characteristics of a smart beam

Figure 4: First Mode response (ζ=0.01)

A numerical case was worked out for a cantilever rectangular cross-section beam, whose characteristics are given

in tab.(1).

The results are relevant to time history of modal amplitudes when no external loads are acting, and all modes have a unit initial amplitude.

it could have been expected.
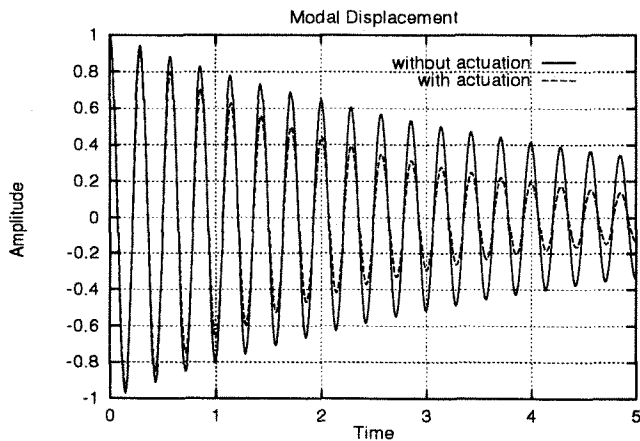
Modal Displacement
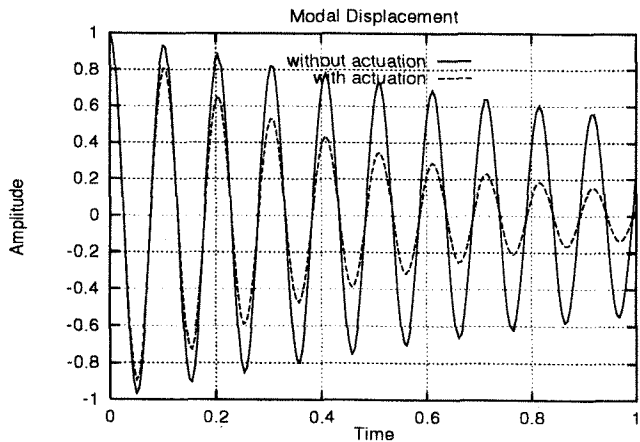

Figure 5: Second Mode response ($\zeta=0.01$)

Figure 6: Third Mode response ($\zeta=0.01$)

Control here extends exactly over the first half of the beam, with a closed-loop gain $G_1=4000$ V/Amp (see App.III(c)). I know that literature is full of more complicated examples, but I want to show here something special.

Figs.(4),(5) and (6) show the evolution in time for a proportional structural damping $\zeta = 0.01$. It is seen that the increase in damping associated with piezoelectric actuations is sensibly increasing with modal frequency, as

Figure 7: First Mode response ($\zeta=0.005$)
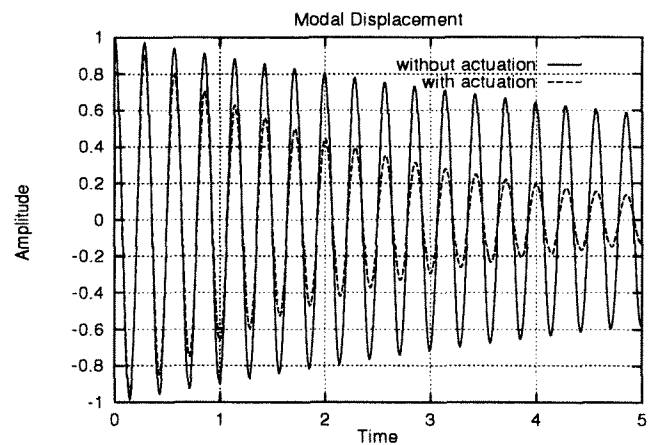
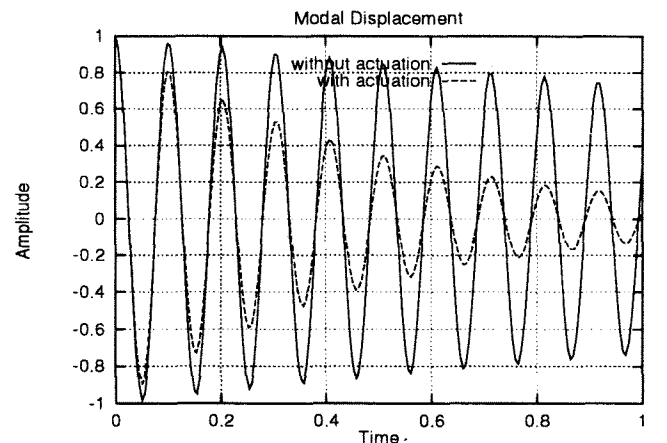Figure 8: Second Mode response ($\zeta=0.005$)

Figure 9: Third Mode Response ($\zeta=0.005$)

Figs.(7),(8) and (9) provide the same results for $\zeta =$

0.005; the resultant damping factor is not much different from the previous case.

5 Illustrative example: a smart plate

For the case of a plate-like structure, we essentially have to follow the same procedure as with the beam. The equations in the frequency domain are the same as (11) and (12); here too we can make a distinction between pin-joint and continuous bondage: in the latter case we ignore the contribution given by C (which, in this case, would be an extensional membrane); the values of the ν's are reported in Appendix V.

There are several excellent papers describing the general behaviour of a smart plate, see [9]. In the time-domain, we still have eq.(17) with the proper expressions of the quantities appearing in it, not reported here for the sake of brevity.

As illustrative example, the open-loop transfer function was worked out for the structure described in tab.(2) (damping factor, missing in the table, is assumed $\zeta = 0.01$), whose general arrangement is shown in fig.(10), see [10]. Shear flexibility and rotary inertia were considered.
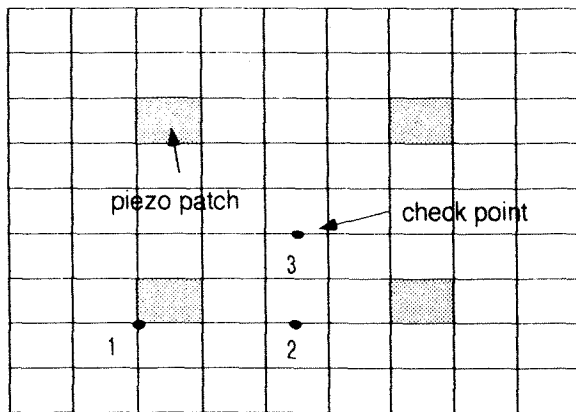

Figure 10: Smart plate scheme (simply supported)

There we have four actuators simmetrically placed, and the transfer function is calculated in the three check
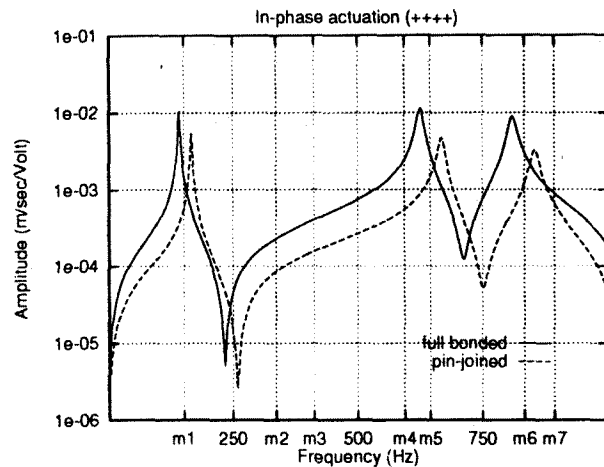

Figure 11: Vertical velocity response of point 1

points showed in the same figure. The four actuators patches are driven by a sinusoidal voltage of constant amplitude that can be positive ($+$) or negative ($-$) for each of them independently.

Figs.(11) and (12) provide results for the points 1 and 3 in the case ($+ + ++$), that means in-phase actuation of all four patches; continuous lines are relevant to full bondage, while dotted lines to pin-joint case. Although the trend is similar, there is a considerable shift in the resonance peaks , i.e., near the resonant frequencies of the uncontrolled plate (indicated in the figures as m1, m2... etc). This is surely due to the influence of adding patch mass and stiffness to the structure.
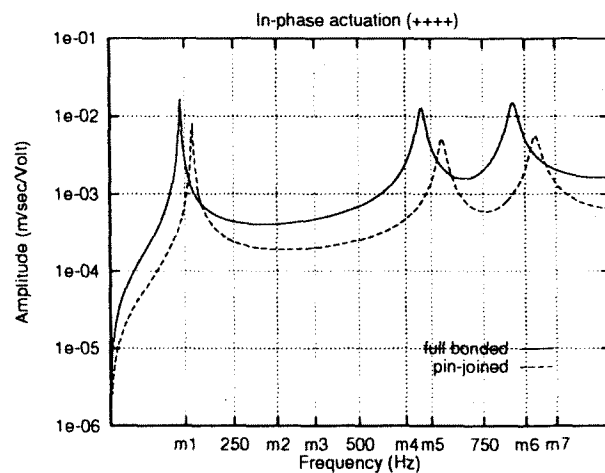

Figure 12: Vertical velocity response of point 2

Fig.(13) provides with similar results for check point no.3.

when the four actuators are driven out-of-phase (+ − +−).

In both cases resonance peaks, as calculated with the full-bondage scheme, are not far from the eigenfrequencies of the host structure.
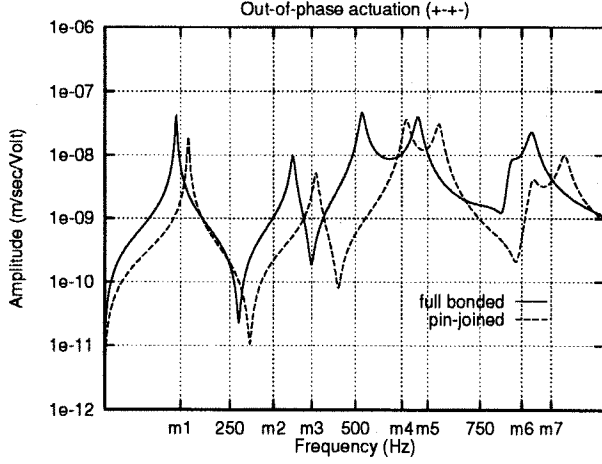

Figure 13: Vertical velocity response of point 3

Characteristics	Al faces	Honeyc. core	PZT
Length (mm)	600	600	66.7
Width (mm)	500	500	55.6
Thickness (mm)	0.2	6.35	0.2
Young's Modulus ($N/m^2 \times 10^9$)	70	1.02	63
Shear Modulus ($N/m^2 \times 10^9$)	26.9	0.434 (x) 0.213 (y)	24.2
Mass Density (kg/m^3)	2700	83.3	7630
PZT constant ($m/volt \times 10^{-9}$)	-	-	166

Table 2: Mechanical Properties (smart plate)

6 Stiffening and damping efficiency

Eq.(17) is very general: it is practically the same for all possible controlled structures, each kind of structure having the proper expressions for the constants, the ma-

trices and the degrees of freedom relevant to it.

It is convenient, first of all, to reduce eq.(17) to a nondimensional form, letting

$$T^2 = \frac{a_m}{a_k} \qquad \tau = \frac{t}{T} \qquad f = \frac{F}{a_m}$$

$$\alpha_h = \frac{a_h}{T a_k} \qquad \alpha_c^0 = \frac{a_c^0}{a_k} \qquad \alpha_c^1 = \frac{a_c^1}{T a_k}$$

we have the standard form:

$$\mathbf{M}^* \ddot{X} + \alpha_h \mathbf{H}^* \dot{X} + \mathbf{K}^* X = \alpha_c^0 \mathbf{L}^* X + \alpha_c^1 \mathbf{L}^* \dot{X} + f \quad (18)$$

So we see that terms containing α_c^0 (direct position feedback control: DPFC) and α_c^1 (direct velocity feedback control: DVFC) play the role of increasing stiffness and damping characteristics of the system.

By inspecting eq.(18) one can pictorially say that forces involved in dynamical equilibrium (through the asterisks matrices) define the respective *shape* (i.e, how they are distributed within the structure), and by nondimensional coefficients, defining the relevant *robustness*. In particular the coefficients α_c^0 and α_c^1 are related to maximum piezoelectric strain and to control gains.

In the frequency domain, eq.(18) reads

$$\left\{ -\omega^2 \mathbf{M}^* + j\omega \left[\alpha_h \mathbf{H}^* - \alpha_c^1 \mathbf{L}^* \right] + \left[\mathbf{K}^* - \alpha_c^0 \mathbf{L}^* \right] \right\} \bar{X} = \bar{f} \quad (19)$$

which provides the closed-loop transfer function, already defined in detail for the beam.

In the frequency domain, it is also possible to make a distinction between controlled and uncontrolled degrees of freedom (see App.VI).

Let us especially concentrate on DVFC. Generally $\mathbf{L}^*$ is a sparse matrix if sensors and actuators are co-located: also, in general it is not symmetric, however, *if its symmetric part is non-positive definite, the closed loop system is energy dissipative.* This means that, if this is the case, DVFC control cannot destabilize or reduce the stability of the system, whatever the choice of the feedback system is. Also, the pole location of the closed loop system will never be placed, in the complex plane, at the right side of their locations for the open loop system.

In order to apply the method, therefore, it should be checked that for the particular choice of actuators and sensor, the matrix is non-positive definite. Although a

general rule does not exist, for the complete matrix $\mathbf{L}^*$, some indication can be found in [11].

The form of eq.(18) is very similar that relevant to other fields of structural dynamics, where one has mass, stiffness, structural damping and other forces. This is, for instance, the case of

- Aeroelasticity

- Flexible bodies in orbit

- Thin structures with in-plane forces (Buckling)

Each of these forces can either stabilize or destabilize the system. The relevant rules have not yet been fully established.

Obviously, it is often convenient to use modal format. If we have the diagonal eigenfrequency matrix, and the modal matrix of the "nude" system, i.e, with $\mathbf{K}^*$ and $\mathbf{M}^*$ only, we can easily write eq.(18) in terms of modal amplitudes, achieving a significant reduction in the size of the differential system (even if, of course, some difficulties are introduced). One of the most serious problems is time-integration schemes, some of which may exhibit conflicting characteristics of accuracy, stability, duration.

7 Torsional control

Torsional control is of great importance in aeronautical structures design, since such structures undergo aeroelastic phenomena, which are deeply connected with torsional stiffness. Therefore the use of smart materials in wing structures is generally confined to the increase in torsional stiffness rather than in damping.

Unfortunately, however, piezoelectric actuators produce extensional strains, not shear strains, so twist control in a beam or a beam-like structure is usually accomplished by orientating the patches at an angle to the beam's longitudinal axis (see fig.14).

Furthermore, practically available materials are isotropic in the plane normal to the poling direction, so that their authority on the torsional movement is rather poor, because it arises only from the bending-twisting coupling effect due to the anisotropic properties of the composite laminate and to the sweep angle of the wing, if any.

A recently proposed alternative technique would consist in using piezoelectric elements, activated in such a way as to produce cross-section warping and, consequently, an angle of rotation, thus improving the torsional stiffness of the structure.
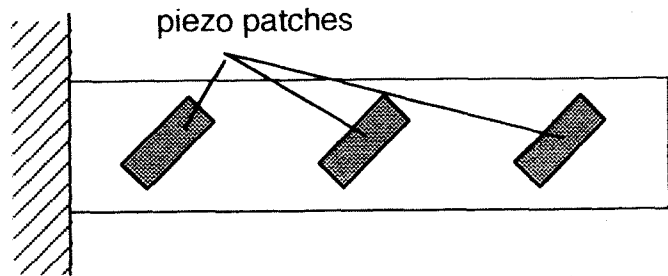

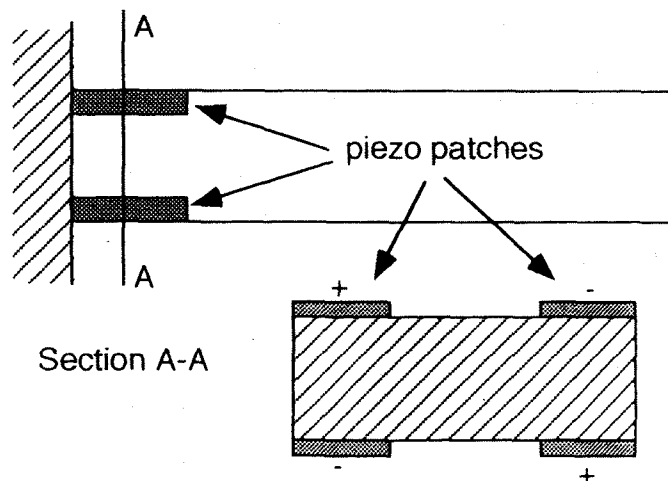Figure 14: Torsional control with diagonal patches

Figure 15: Torsional control using bimoment

A typical case was worked out in [12]: the results obtained with DAP elements control (i.e., patches at some angle with the beam axis) are compared with results achieved using a bimoment due to opposite piezoelectric stresses in a logitudinal element (see fig.15).

The relevant results can be read in the original paper: suffice here to say that the bimoment control in this case induces section rotations almost three times greater than with DAP approach; however, in both cases the rotation control is very small, as confirmed by the analysis performed in Appendix VII.

8 Aeroelastic applications

The problem of the aeroelastic behaviour of an aircraft is one of the major concerns in aeronautical design. Due to the high flexibility of their use, composite components can prevent, or delay, undesired phenomena, such as divergence, flutter, aileron reversal, and/or unwanted changes in aerodynamic loads. In dynamical problems, however, simple use of composites may not be sufficient, or viable. Thus, piezoelectric devices could be envisaged. When dealing with aeroelastic problems, adequate modeling for structural and aerodynamic behaviour should be available.

For the former, there exist a large number of models, starting from simple analytical solutions to sophisticated finite element approaches: since, however, in Aeroelasticity *global* rather than *local* quantities are of interest, classical methods may need some updating.

For aerodynamics, in principle, unsteady formulations should be used, since quasi-unsteady aerodynamics might give poor results. Thus, in aeroelastic control, new matrices and relevant coefficients (typically related to dynamic pressure, made somehow nondimensional) enter the loop described by eq.(17). Such matrices generally play a role similar to $DPFB$ and $DVFB$ control.

A reasonably complete treatment of the problem is given in [13] to which the reader is referred. We will confine ourselves here to illustrate the numerical example contained in it.

consisting of 20 layers was considered, fig.(16); the first three upper and lower are piezoelectric: the first two are used as actuators, while the third one acts as a sensor. Maximum attainable free strain is 180 $\mu\varepsilon$: $DVFC$ only is present, with a gain of 1000 V/A.

The structural model of the wing is an equivalent plate, where chordwise and spanwise variations of structural parameters can be accounted for: displacements are modelled by a chordwise power series and, for each term, by spanwise beam-like shape functions. In this way, global quantities are the unknowns [14].

As far as aerodynamics is concerned, piston theory in supersonic flight was considered, at $M=1.5$, and dynamic pressure of 5400 N/m^2. The wing has an aspect ratio of 10, and positive sweep angle of 45 degrees.

With this choice of actuators and sensors, the symmetric part of control matrix to be non-negative is verified, so we are sure that piezos act as dampers. Each of the active elements, for a total of 3 near the clamped ends, is assumed to coincide with one of the 16 spanwise elements taken for the structural model.

The results presented here are relevant to the case of a gust corresponding to a unit angle of attack for two models:

(i) step gust

(ii) one-minus-cosine gust
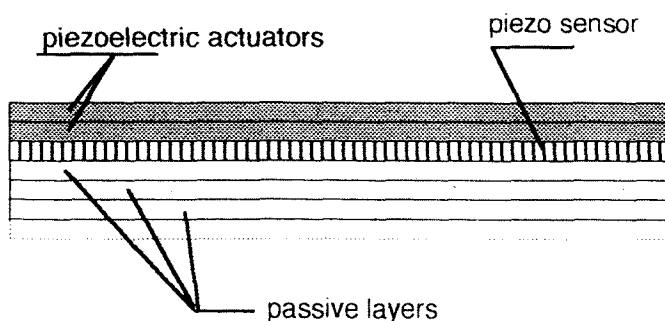
Both have a duration of 20 seconds.

Figure 16: Wing piezoelectric laminate

The structure here considered is a cantilever wing. In order to apply the proposed method, a wing active element
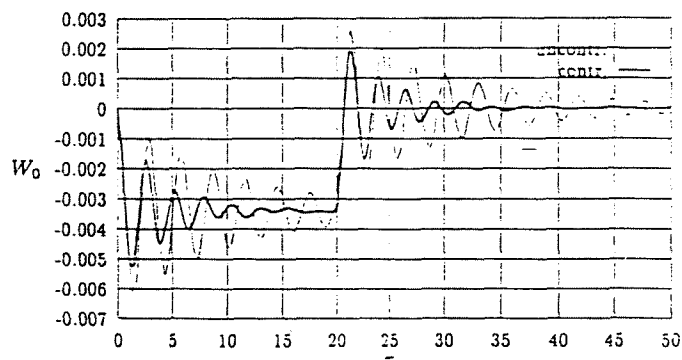

Figure 17: Tip displacement response to gust (i)

Fig.(17) shows the time history of flexural (average) tip displacement, made nondimensional with respect to the wing length.
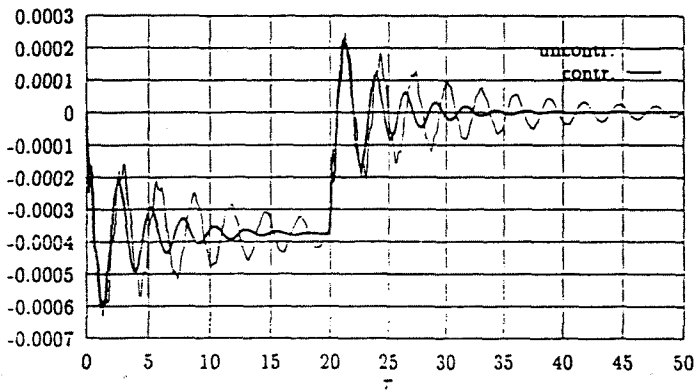
damping is obtained, due to the fact that there is a higher aerodynamic damping.

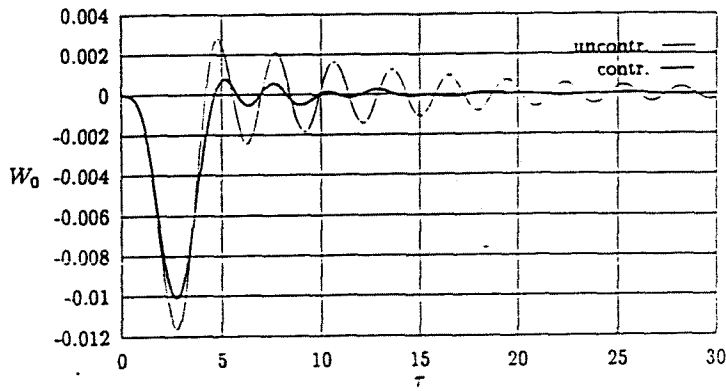Figure 18: Tip torsional response to gust (i)

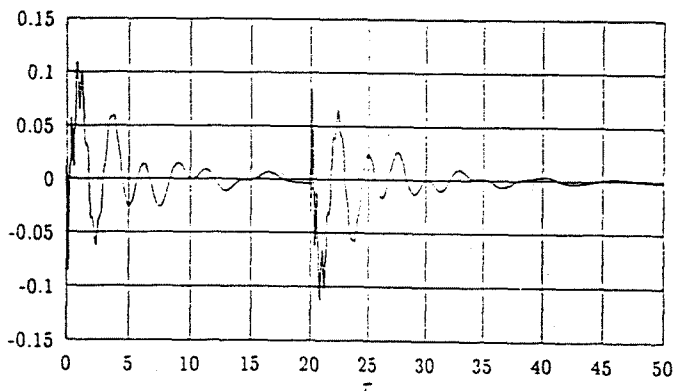Figure 20: Tip displacement response to gust (ii)

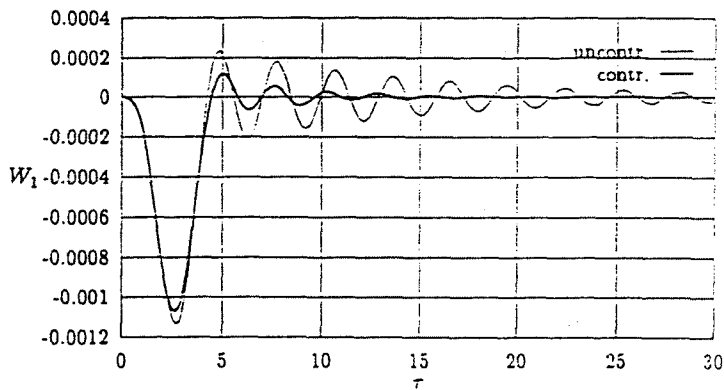Figure 19: Applied voltage during gust (i)

Figure 21: Tip torsional response to gust (ii)

Fig.(18) is relevant to the tip rotation. The results clearly show the increase of damping in the system due to $DVFC$ control.

A physical limitation exists to the maximum voltage (or, better, to the electric field) that can be applied to a piezoelectric lamina, due to the fact that the electric field should not exceed the depoling field, which, for the case under concern, has been taken as 10^5 V/m.

This condition has been checked, fig.(19), where the electric field (made nondimensional with respect to E_{max}) is shown. Similar results are shown in figs.(20) and (21) for case (ii), where, however, a fairly smaller percent of

9 Static control of lifting surfaces

Control of lifting surfaces could, in principle, be achieved through the two different approaches described in art.7. Piezo-patches imbedded in the wing composite layup or spanwise actuators replacing spar elements could provide an apparent increase in torsional stiffness, since they are capable of inducing torsional deformations such as to counteract the effects of aerodynamic torques [15][16].

The problem is studied in great detail in [17] [18], where a complete solution is provided for the case described in

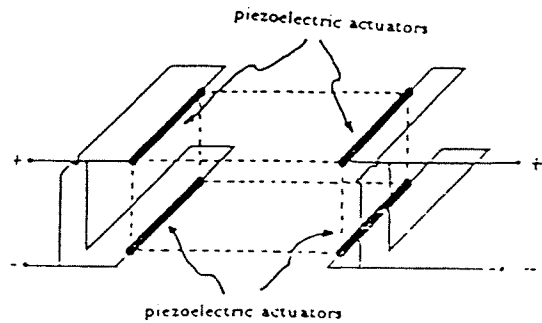fig.(22)(axial actuators) and in fig.(23)(embedded actuators).
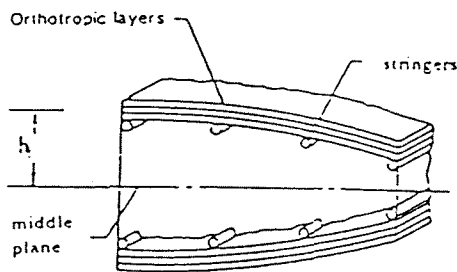

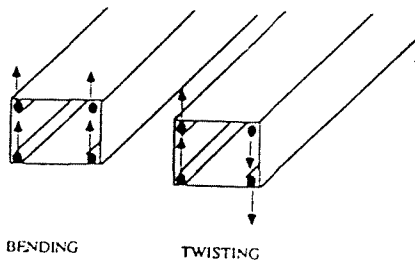Figure 22: Actuator bay configuration

Figure 23: Wing box section

Figure 24: Actuator torsion and bendig effects

In the first case, on account of the coefficients d_{33} there will be an elongation of the stringers: thus, if the elements 1-3 have positive voltage and the elements 2-4 a

negative one, there will be an antisymmetric, or twisting movement (see fig.(24), right), whereas for 1-2 positive and 3-4 negative there will be a symmetric, or bending motion (see fig.(24), left). On the contrary, the effect of embedded layer is principally due to anisotropy and angle-of-sweep effects.
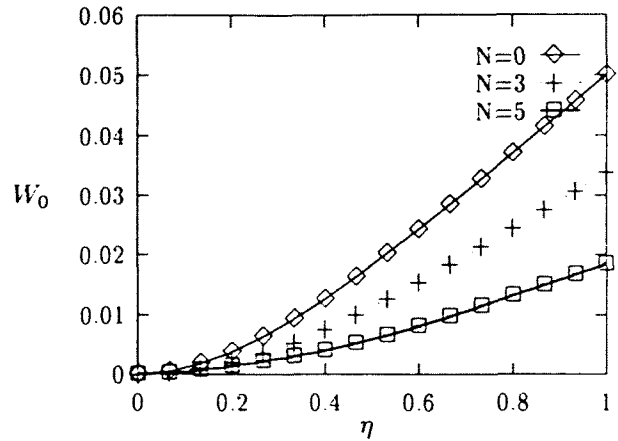

Figure 25: Center line elastic response with N activated piezoelectric
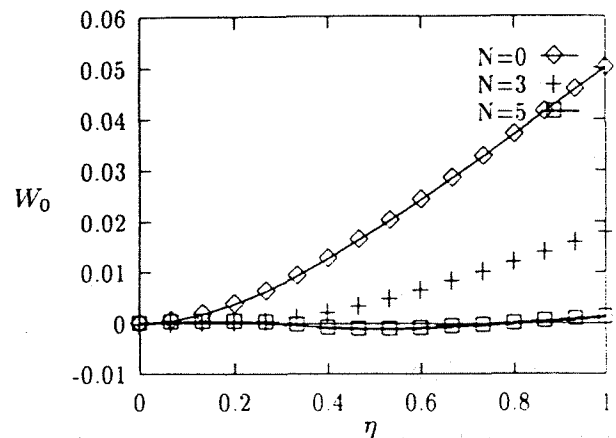
Figure 26: Center line elastic response with N activated ribs

Figs.(25) and (26) show the center line vertical displacement response to aerodynamic loads for $U_\infty = 200 \ m/s$, on a wing with $\Lambda = -30°$ in both cases (axial actuators and embedded actuators) with different number of active elements.

Figs.(27) and (28) show similar results for tip twisting angle. It should be said, however, that the results are not very realistic, since no check on the upper limit for

V_{max} was made. Further work should include this limitation, and then results are likely to change.
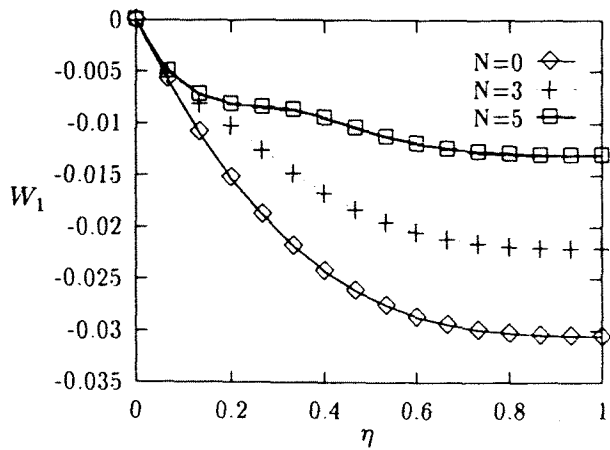

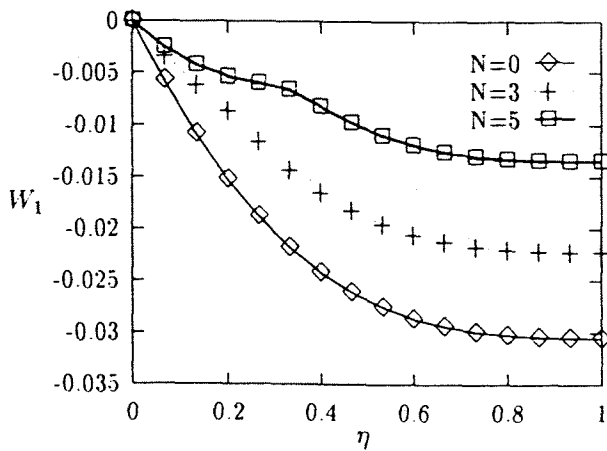Figure 27: Torsion elastic response with N activated piezoelectric

Figure 28: Torsion elastic response with N activated ribs

10 Active control of wave propagation

We consider here a one-dimensional, indefinite (but not necessarily infinite), structure, referred to a longitudinal x-axis. A good example of interest in aerospace engineering is a shell wing or a fuselage, where, also, geometric characteristics are dependent on x. The structure is considered in dynamic conditions and we shall conduct a frequency domain analysis, App.IX (see also [19] [20] [21].

The conditions of the structure are defined through a state vector $Y(x,\omega)$ which includes not only displacements but internal forces too; f.i, for a simple beam, Y consists of four variables: lateral displacement, rotation, internal bending moment and internal shear force. For a shell wing the situation is much more complicated, [22]. It is well known that, in such approach, it is possible to define a propagation function $P(x_0, x_1, \omega)$ relating the state Y_0 at a station x_0 to the state Y_1 at a station x_1. This is practically equivalent to solve the structural problem with initial rather than with end conditions. This is, in general a non-natural way to solve structural problems, and it could easily be seen that it would be a non practicable, although formally correct way of operation. It should be borne in mind, however, that this is not the aim of wave propagation analysis, which seeks relationships between states independently of the circumstances which have produced such states (forces, constraints, environment).

State can also be defined by means of "waves", corresponding to eigenmodes of propagation, which are not the eigenmodes of the structure, and which are an index of how energy is transferred, and how the state is travelling, along the structure, in the two directions of the reference axis.
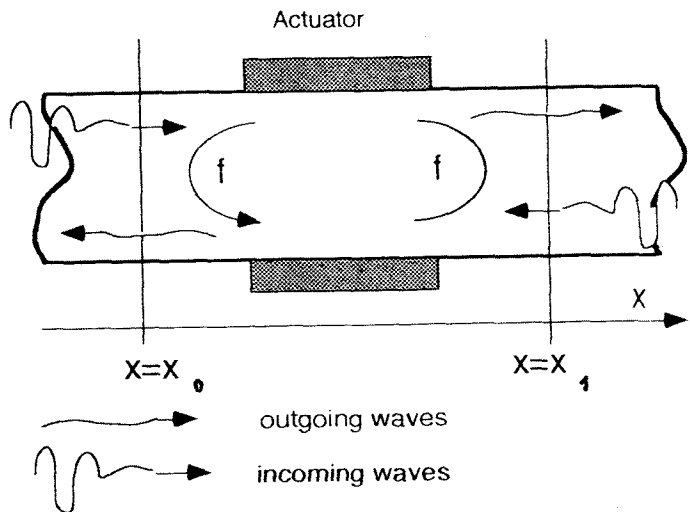

Figure 29: Wave propagation control

Let us now consider, fig.(29), a portion of structure between two sections: here we can define "entering waves" and "outgoing waves" and range each group in a vector.

Furthermore, there will be, in general, some discontinuity in the element: for our purposes, the only discontinuities of interest are forces, if any, applied between the two sections. With this in mind, the basic relationship between outgoing w_{out} and incoming w_{in} waves is:

$$w_{out} = S(x_0, x_1, \omega)\, w_{in} + \psi f \qquad (20)$$

where $S(x_0, x_1, \omega)$ is the so-called *dispersion function*, ψ the load-generating function, and f is the applied force. For control purposes we have the situation described in fig.(29). Let us assume we have waves propagating along positive x, and we want to control vibrations somewhere outside the region $\mathcal{R}$ (active region), defined by sections x_0 and x_1. At such sections we put two sensors (not necessarily piezo- or anyhow smart) and an actuator inside the region. In order to design our control we must produce forces

$$f = G(\omega)\, m(\omega) \qquad (21)$$

where $G(\omega)$ is the gain-matrix and $m(\omega)$ is an observed vector, related to waves amplitude by:

$$m(\omega) = M_{in} w_{in} + M_{out} w_{out} \qquad (22)$$

where M_{in} and M_{out} are appropriate matrices. Combining the above equations we have the closed-loop dispersion function:

$$\bar{S} = [I - \psi G(\omega) M_{out}]^{-1} [S + \psi G(\omega) M_{in}] \qquad (23)$$

Therefore, through proper selection of the matrix gain, we can obtain the requested closed loop dispersion function.

In principle, if n is the order of the state Y, $[n \times n]$ is the order of the dispersion function, so $n \times n$ parameters could be controlled through. In practice, however, only a much smaller number of d.o.f. is measurable, and only a much smaller number of control forces is available.

Fig.(29) (from [21]) is relevant to the case of a beam; although many choices could be possible, here, the choice was made of taking the mean line curvature as the observed quantity. As far as gains are concerned, only one parameter was taken, so the matrix $G(\omega)$ reduces to a

scalar $g(\omega)$ and, consequently, only one of the components of the closed loop dispersion function can be chosen. Also, the desired control was designed in such a way that the outgoing wave was cancelled. For this purpose, a simple expression for the gain as a function of ω can be obtained, as represented in figs.(30) and (31).
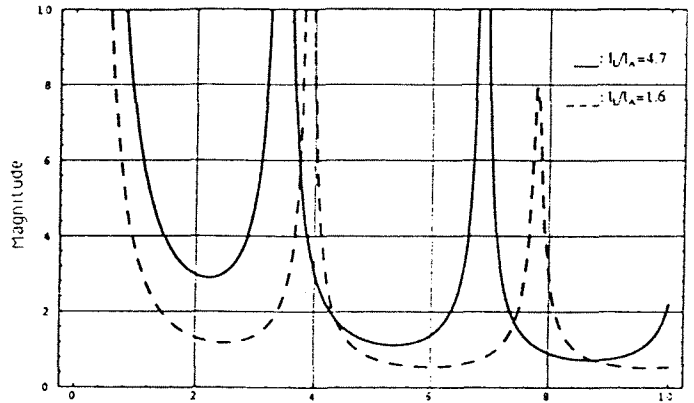
Figure 30: $|g(\omega)|$ vs. dimensionless frequency
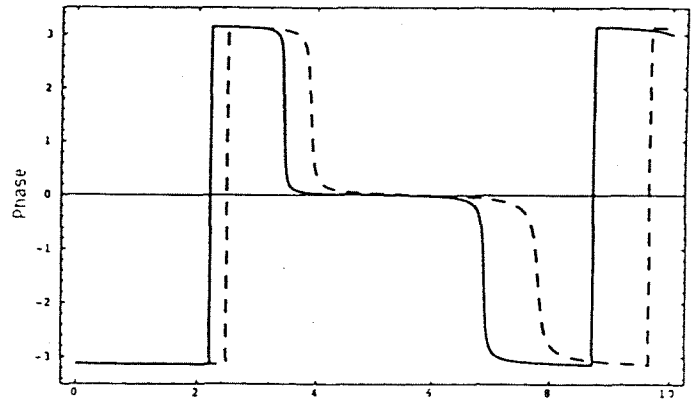
Figure 31: phase of $g(\omega)$ vs. dimensionless frequency

11 Experimental work

Experimental results are of prime importance in our field. Our Department is deeply involved in an ESA-sponsored program which is, however, at its first steps in the Laboratories of San Diego State University. I hope to be able to give a full report on the results at the time of the final version and of the presentation in Sorrento.

12 Conclusions and future work

The conclusions are already contained in what I have said above. I must confess to feel a little frustrated on account of the limitations associated with small amplitudes requirements I tried to illustrate several times. In certain areas smart structures could prove excellent, but much has to be done in terms of reliability, confidence, affordability, production technology. In my opinion, much has to be done also to understand basic priciple of control, optimization of sensors and actuators position, strategies, etc.

From our viewpoint the goal we shall try to reach is to acquire a better knowledge of what seems to be today the needs of a modern society: better materials, better control, better experience. And use of mathematical models on realistic structures, what we are currently doing.

13 Acknoledgements and thanks

14 Dedicated to John Green

This was the best english I could afford. I hope it is not too bad for a non English born senior citizen, is it ?

A Appendix I

In eqs.(1) $\sigma = [\sigma_1, \sigma_2, \sigma_3, \tau_{23}, \tau_{13}, \tau_{12}]^T$ is the vectorized stress-tensor (with the convention $\sigma_4 = \tau_{23}$, $\sigma_5 = \tau_{13}$ and $\sigma_6 = \tau_{12}$), $p(x_1, x_2, x_3, t)$ is the external force per unit volume and ∇ is the differential operator transforming σ into body stress-forces:

$$\nabla = \begin{bmatrix} \frac{\partial}{\partial x_1} & 0 & 0 & 0 & \frac{\partial}{\partial x_3} & \frac{\partial}{\partial x_2} \\ 0 & \frac{\partial}{\partial x_2} & 0 & \frac{\partial}{\partial x_3} & 0 & \frac{\partial}{\partial x_1} \\ 0 & 0 & \frac{\partial}{\partial x_3} & \frac{\partial}{\partial x_2} & \frac{\partial}{\partial x_1} & 0 \end{bmatrix} \quad (24)$$

Furthermore, $q(x_1, x_2, x_3, t)$ is the force per unit surface, applied to the boundary $\partial \mathcal{B}$ and the finite operator R is given by:

$$R = \begin{bmatrix} \alpha_1 & 0 & 0 & 0 & \alpha_3 & \alpha_2 \\ 0 & \alpha_2 & 0 & \alpha_3 & 0 & \alpha_1 \\ 0 & 0 & \alpha_3 & \alpha_2 & \alpha_1 & 0 \end{bmatrix} \quad (25)$$

where α_1, α_2, α_3 are the director cosines of the outer normal to $\partial \mathcal{B}$.

In eqs.(2) ε denotes the vectorized strain tensor

$$\varepsilon = [\varepsilon_1, \varepsilon_2, \varepsilon_3, \gamma_{23}, \gamma_{13}, \gamma_{12}]^T$$

S^E is the [6 × 6] elasticity tensor for constant E, d^T is the [3 × 6] piezoelectric matrix. Choosing the intrinsic coordinate axes according to symmetry, that exists in certain classes of piezoelectric materials, the piezo matrix reads:

$$d^T = \begin{bmatrix} 0 & 0 & 0 & 0 & d_{15} & 0 \\ 0 & 0 & 0 & d_{24} & 0 & 0 \\ d_{31} & d_{32} & d_{33} & 0 & 0 & d_{36} \end{bmatrix} \quad (26)$$

Finally, E is the vector of the electric field, D is the electrical displacement, P^σ is the [3 × 3] electric permissivity tensor for constant σ.

The above expressions hold for three dimensional elements. For two dimensional elements, the vectors σ and

ε simply reduce to

$$\sigma = [\sigma_1, \sigma_2, \tau_{12}]^T$$
$$\varepsilon = [\varepsilon_1, \varepsilon_2, \gamma_{12}]^T$$

In the matrices ∇ and R columns 3, 4, 5 and row 3 must be deleted.

For one dimensional elements we have

$$\sigma = [\sigma_1]$$
$$\varepsilon = [\varepsilon_1]$$
$$\nabla = \partial/\partial x$$
$$R = [\alpha_1]$$

where α_1 reduces to unity, on account of normality condition.

B Appendix II

In general, in a piezo patch, $E_j = const$, so the first term in Eq.(6) is vanishing. As far as the other term is concerned, we set $w(x_1, x_2, x_3) = N_j(x_1, x_2, x_3)X_j$, where the N_j's contain the shape function assumed in the f.e.m. approach. In a rectangular flexural plate, where only the tranverse displacement $w_n(x_1, x_2, x_3)$ is of interest, we have 3 d.o.f. for each node, and using a four-node element a total of $[4 \times 3]$ d.o.f; so N_j is a (well-known) $[1 \times 12]$ matrix; use of intermediate nodes may increase the value 12, as well as consideration of shear flexibility. In an extensional membrane, we have in-plane displacements $u = u(x_1, x_2, x_3)$, $v = v(x_1, x_2, x_3)$, and, for bilinear shape functions, a size $[2 \times 8]$ of the matrices N_j. Thus, for the matrix appearing in eq.(7) we have now

$$P_j = \int_{\partial \mathcal{B}_j} N_j^T R(H\mathsf{d}) \, d(\partial \mathcal{B}_j) \tag{27}$$

Clearly, the integration expressed by the above equation is to be extended only to the positions of the element which are occupied by piezoelectric materials, since, elsewhere, $\mathsf{d} = 0$.

C Appendix III

(a) Consider the piezo patch of fig.(2) as an extension bar, with:

$$A_p = \text{cross section}$$
$$E_p = \text{modulus of elasticity}$$
$$L_p = \text{lenght}$$
$$\mu_p = \text{mass per unit lenght}$$
$$u = \text{axial displacement}$$

where the subscript "p" refers to piezoelectric. For the equation of motion in the frequency domain we have

$$\frac{d^2 \bar{u}}{d\xi^2} + \lambda_p^2 \bar{u} = 0 \tag{28}$$

where

$$\lambda_p^2 = \omega^2 \frac{\mu_p L_p^2}{E_p A_p} \qquad \xi = x/L_p \qquad \bar{u} = u/L_p$$

Integration of eq.(28) with the boundary conditions $\bar{u}(0) = \bar{u}_0$ and $\bar{u}(1) = \bar{u}_1$ yields:

$$\bar{u} = \bar{u}_0 \frac{\sin[p_p(1-\xi)]}{\sin(p_p)} + \bar{u}_1 \frac{\sin(p_p \xi)}{\sin(p_p)} \tag{29}$$

In order to compute end-forces on the bar, we can apply the one-dimensional version of the first of eqs.(2), obtaining:

$$\bar{N}_0 = \frac{E_p A_p}{L_p} \left[p_p \left(\bar{u}_1 \csc(p_p) - \bar{u}_0 \cot(p_p) \right) - \frac{L_p d_{31}}{h_p} V \right]$$

$$\bar{N}_1 = \frac{E_p A_p}{L_p} \left[p_p \left(\bar{u}_1 \cot(p_p) - \bar{u}_0 \csc(p_p) \right) - \frac{L_p d_{31}}{h_p} V \right] \tag{30}$$

where h_p represents the piezoelectric bar thickness (negligible with respect to beam height). Denoting by z_p the distance of the patches from the beam axis, we easily obtain the coefficients appearing in eqs.(9) and (10):

$$c_{00} = -c_{11} = -2z_p^2 \frac{E_p A_p}{L_p} p_p \cot(p_p)$$

$$c_{01} = -c_{10} = -2z_p^2 \frac{E_p A_p}{L_p} p_p \csc(p_p)$$

$$\nu_0 = -\nu_1 = -2z_p^2 \frac{E_p A_p}{h_p} d_{31}$$

(b) Consider a beam of lenght L_a, flexural stiffness $E_a I_a$, mass per unit length μ_a and divide it into n elements. Let $\delta = \frac{1}{n}$. The cases of nonuniform beam or nonuniform lenghts are easily treated, keeping for the above quantities a reference, or a mean value, and considering variation in the individual mass, stiffness, control elements. For the transverse displacement $w = L_a \bar{w}$ in one element (x_{j-1}, x_j), we can use the classical cubic approximation, and write:

$$\bar{w} = X_j^T \Psi$$

where X_j^T are the d.o.f of the j-th element $(\bar{w}_0, \theta_0, \bar{w}_1, \theta_1)$ and Ψ is the vector of the shape functions:

$$
\begin{aligned}
\psi_1(\xi) &= 1 - 3\xi^2 + 2\xi^3 \\
\psi_2(\xi) &= (\xi - 2\xi^2 + \xi^3)\delta \\
\psi_3(\xi) &= -3\xi^2 - 2\xi^3 \\
\psi_4(\xi) &= (-\xi^2 + \xi^3)\delta
\end{aligned}
$$

with $0 \leq \xi \leq 1$.
So, the kinetic energy in the element is written:

$$T = \frac{1}{2} \int_{x_{j-1}}^{x_j} \mu_a \left(\frac{\partial w}{\partial t} \right)^2 dx = a_m \dot{X}_j^T M_j^* \dot{X}_j \qquad (31)$$

where:

$$
\begin{aligned}
M_j^* &= \int_0^1 \Psi \Psi^T d\xi \\
a_m &= \mu_a L_a^2
\end{aligned}
$$

For the elastic potential energy:

$$\mathcal{E} = \frac{1}{2} \int_{x_{j-1}}^{x_j} E_a I_a \left(\frac{\partial^2 w}{\partial x^2} \right)^2 dx = a_k X_j^T K_j^* X_j \qquad (32)$$

where:

$$
\begin{aligned}
K_j^* &= \int_0^1 \frac{\partial^2 \Psi}{\partial \xi^2} \frac{\partial^2 \Psi}{\partial \xi^2}^T d\xi \\
a_k &= \frac{E_a I_a}{L_a}
\end{aligned}
$$

The matrices M^*, K^* of eqs.(31) and (32) are then assembled version of M_j^* and K_j^*.
Note, however, that the above treatment is greatly simplyfied. For a better understanding of piezo-patch interaction, see [23].

(c) The scheme of the layout for the piezo of the beam is considered in fig.(32).
The piezoelectric moment for a $1V$ voltage and the charge collected on the sensor because of deformation are respectively (see App.IV(b)):

$$
\begin{aligned}
M_p &= 2 z_p d_{31} E_p b \\
Q_p &= z_p d_{31} E_p b (\theta_1 - \theta_0)
\end{aligned}
$$

and, so, if we have gains G_0 and G_1 for Q_p and $\dot{Q}_p$:

$$
\begin{aligned}
M_c &= M_p V = M_p \left(G_0 Q_p + G_1 \dot{Q}_p \right) = \\
&= (2 z_p d_{31} E_p b)(z_p d_{31} E_p b) \left(G_0 Q_p + G_1 \dot{Q}_p \right) = \\
&= 2(z_p d_{31} E_p b)^2 \left[G_0(\theta_1 - \theta_0) + G_1 \left(\frac{d\theta_1}{dt} - \frac{d\theta_0}{dt} \right) \right] = \\
&= a_c^0 (\theta_1 - \theta_0) + a_c^1 \left(\frac{d\theta_1}{dt} - \frac{d\theta_0}{dt} \right)
\end{aligned}
$$

where

$$
\begin{aligned}
a_c^0 &= 2 G_0 (z_p d_{31} E_p b)^2 \\
a_c^1 &= 2 G_1 (z_p d_{31} E_p b)^2
\end{aligned}
$$

that are the coefficients appearing in eq.(17). Considering the j-th element of the beam

$$
\begin{aligned}
(\theta_1 - \theta_0)_j &= L_j X \\
\left(\dot{\theta}_1 - \dot{\theta}_0 \right)_j &= L_j \dot{X}
\end{aligned}
$$

where X is the vector of all the beam d.o.f., thus assembling the element matrices L_j, one obtains the global matrix L^*.
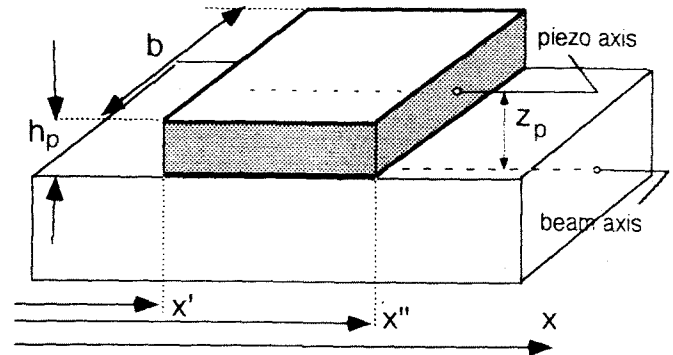

Figure 32: Piezoelectric patch layout

D   Appendix IV

(a) For a structure having modal format defined by frequencies ω_r and modes $W_r(\vec{x})$, where $\vec{x}$ is the vector defining positions, we have

$$G(\vec{x}, \vec{x}_1) = \sum_{r=1}^{\infty} \frac{W_r^T(\vec{x})W_r(\vec{x}_1)}{\omega^2 - \omega_r^2} \qquad (33)$$

In the frequency domain, damping effect is often accounted for by considering a complex modulus $E = E_0(1+j\eta)$, which is equivalent to set in eq.(33) $\omega_r^2(1+j\eta)$ instead of ω_r^2: so we have the complex expression of Green's influence matrix

$$G' + jG'' = \sum_{r=1}^{\infty} \frac{W_r^T(\vec{x})W_r(\vec{x}_1)}{\omega^2 - \omega_r^2(1+j\eta)} \qquad (34)$$

(b) In the one-dimensional case under concern, the first of eqs.(2), with respect to σ reads:

$$\sigma_1 = E_p \left[z_p \frac{\partial \theta}{\partial x} - d_{31} \frac{V}{h_p} \right]$$

where, using previously defined notations, z_p is the distance of the patch from the beam axis and h_p is the thickness of the patch. Thus the piezoelectric bending moment is :

$$M_p = E_p d_{31} \frac{V}{h_p}(b\, h_p)2z_p = 2z_p d_{31} E_p b\, V \qquad (35)$$

where b = width of the beam and of the patch (the thickness h_p is assumed negligible as compared to z_p).
For the sensor, co-located with the actuator, the second of eqs.(2) yields:

$$D = d_{31}\sigma_1|_{V=0} = d_{31}E_p z_p \frac{\partial \theta}{\partial x}$$

So, the electric charge collected is :

$$\begin{aligned} Q_p &= \iint D\, dS = b \int_{x'}^{x''} D\, dx = \\ &= z_p d_{31} E_p b \int_{x'}^{x''} \frac{\partial \theta}{\partial x} dx = z_p d_{31} E_p b\ (\theta_1 - \theta_0) \end{aligned}$$

E   Appendix V

A laminated piezoelectric wing plate is made of several piezoelectric as well as non-piezoelectric laminae. In general each lamina is oriented at an angle α with respect to a global reference system. Introducing the stress-matrix transformation:

$$T(\alpha) = \begin{bmatrix} c^2 & s^2 & -2sc \\ s^2 & c^2 & 2sc \\ sc & -sc & c^2 - s^2 \end{bmatrix} \qquad (36)$$

using, for brevity, the notation $c = \cos(\alpha)$ and $s = \sin(\alpha)$, we obtain the constitutive equation relating σ to ε as:

$$\sigma = H\varepsilon - rE \qquad (37)$$

where

$$\begin{aligned} H &= T^T \overline{H} T \\ r &= T^T \overline{H} \mathbf{d} \\ E &= [0\ 0\ E_3]^T \end{aligned}$$

with $\overline{H}$ representing the orthotropic second-order tensor of elasticity. Now, if we compute the bending and twisting moments, we obtain

$$\begin{bmatrix} M_1 \\ M_2 \\ M_3 \end{bmatrix} = \int_{-h/2}^{+h/2} z\sigma dz = D\kappa + \nu V$$

denoting by κ the curvature vector and by D the stiffness matrix of the plate,

$$D = \frac{1}{3} \sum_{j=1}^{N} (z_j^3 - z_{j-1}^3)H^{(j)} \qquad (38)$$

where z_j and z_{j-1} are the upper and lower limits of the j-th layer, $H^{(j)}$ is the matrix relevant to the layer. Indicating with h_j the thickness of j-th patch, the piezoelectric matrix ν_j is given by:

$$\nu = -\frac{1}{2} \sum_{j=1}^{N} (z_j^2 - z_{j-1}^2) \frac{r^{(j)}}{h_j} \qquad (39)$$

From above, it is seen that the actuating effect of piezo laminae or patches is to introduce bending or twisting moments of value (39) acting on the plate at the sides

of the patch. For a rectangular, orthotropic element, we only have bending moments acting parallel to the patch sides.

F Appendix VI

Let us define X_1 as the vector containing the controlled d.o.f of a structure and X_2 as the vector of the uncontrolled ones; partitioning the matrices appearing in (19) and indicating with indices 1 and 2 the part of each matrix corresponding respectively to X_1 and X_2 we can write:

$$\mathbf{J}_{jk} = \left\{ -\omega^2 \mathbf{M}_{jk}^* + j\omega\alpha_h \mathbf{H}_{jk}^* + \mathbf{K}_{jk}^* \right\} \quad j,k = 1,2$$

and the equation (19) becomes:

$$\left[\mathbf{J}_{11} - j\omega\alpha_c^1 \mathbf{L}_{11}^* - \alpha_c^0 \mathbf{L}_{11}^* \right] \bar{X}_1 + \mathbf{J}_{12}\bar{X}_2 = f_1$$
$$\left[\mathbf{J}_{21} - j\omega\alpha_c^1 \mathbf{L}_{21}^* - \alpha_c^0 \mathbf{L}_{21}^* \right] \bar{X}_1 + \mathbf{J}_{22}\bar{X}_2 = f_2$$

Elementary matrix algebra allows to eliminate $\bar{X}_2$ between the two foregoing equations leaving only $\bar{X}_1$ as degrees of freedom. This has tacitly been done in the example concerning the beam, where rotation only were controlled.

G Appendix VII

We consider a simplified model of a shell-wing structure, as showed in fig.(33), under the action of a bimoment at the free end, consisting of four equal and opposite forces of intensity N_1. On account of symmetry, we only have rotations $\theta = \theta(y)$ and doubly antisymmetric axial displacement $v = L\bar{v}$. By writing the equations of equilibrium and of elasticity of the stringers and of the ribs and introducing the adimensional coordinate $\eta = y/L$, we have [24]:

$$\frac{d^2\bar{v}}{d\eta^2} + \frac{\delta GS}{2EA}\frac{d\theta}{d\eta} - \sigma\frac{2GL^2}{EA}\bar{v} = 0$$
$$\frac{d^2\theta}{d\eta^2} - \frac{4\delta L^2}{\sigma S}\frac{d\bar{v}}{d\eta} = 0 \qquad (40)$$

with the boundary conditions:

$$\eta = 0 \quad \rightarrow \quad \bar{v} = \theta = 0$$

$$\eta = 1 \quad \rightarrow \quad \frac{d\theta}{d\eta} - \frac{4\delta L^2}{\sigma S}\bar{v} = 0, \quad \frac{d\bar{v}}{d\eta} = \frac{N_1}{EA}$$

and the above symbols:

$$\beta_h = \frac{2t_h}{a} \qquad \beta_v = \frac{2t_v}{c}$$
$$\delta = \beta_h - \beta_v \qquad \sigma = \beta_h + \beta_v$$

A = stringers section $S = a \cdot c$
E = Young's modulus G = Shear modulus

From the above equations one obtains easily:

$$\theta(\eta) = \mu\frac{N_1}{EA}\frac{\cosh(\gamma\eta - 1)}{\gamma^2\cosh(\gamma)}$$
$$\gamma^2 = \frac{8GL^2}{EA}\frac{\beta_h\beta_v}{\beta_h + \beta_v}$$
$$\mu = \frac{4\delta L^2}{\sigma S}$$

If N_1 is the force provided by an actuator, then $\tau = N_1/EA$ is the relevant strain. In current aeronautical structures γ is a relatively high number ($\simeq 15$), μ depends on the aspect ratio and on the wing shape and δ/σ is of the order of 1.

Made these cosiderations, if we take the value $\tau = 300\mu\varepsilon$ as maximum admittable strain, with $\gamma = 15$ and $\mu = 500$, we obtain $\theta(1) \simeq 0.67 \cdot 10^{-3}\ rad$, i.e. $\simeq 0.4^o$, a very small number.
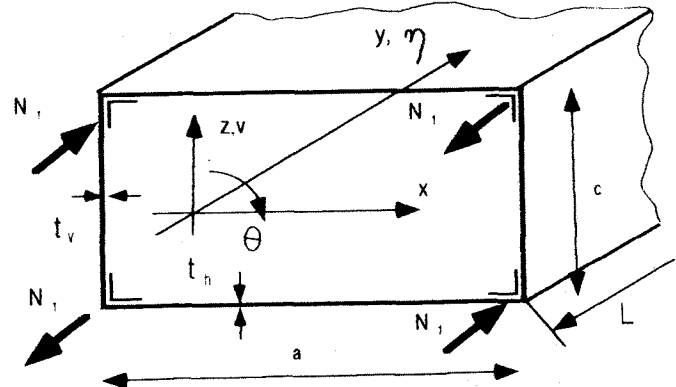

Figure 33: Simplified model of shell-wing

H Appendix VIII

We shall confine ourselves here to list some of the major fields of application of Smart Components (Structures,

Materials, Systems) in Aerospace Technology. A great deal of information is taken from [4]:

(i) Application of Smart Technology to helicopters has proven successful, see also [26]. Some major achievements were relevant to isolation of helicopter fuselages from blade passing noise. Recently also high frequency transmission is satisfactory controlled through use of magnetostrictive actuators.

(ii) Control of cabin noise is one of the fields in which substantial successes have been obtained, and in which a good deal of improvements is expected: again the reason of the success lies in the small amplitudes involved.

(iii) In the propulsion field, distributed actuators placed around the surface of the nacelle intake have allowed to obtain a substantial reduction of noise coming from fan blades.

(iv) As well known, acoustic loads at take off of a rocket are one of the major concern for designers, and here too alleviation is possible.

(v) Coming back to Aeroelasticity, it seems possible to reduce or even suppress tailplane or fin buffeting by incorporating actuators in their structure.

(vi) Acoustic fatigue also might be one of the fields of interest, with some hopes for increasing lifetimes of sandwich panels, widely used also in Space Structures.

(vii) Isolation of avionic equipment, for any aerospace vehicle, from all sources of vibration and shock would be of great benefit, and possibly allow to use cheaper components.

(viii) In space application, antennas deployment system could be one of the prime candidates for use of Smart Structures.

I Appendix IX

In general, for a one-dimensional structure in the frequency domain, the equation of the state Y reads with $2n$ degrees of freedom:

$$\frac{dY(x,\omega)}{dx} = A(x,\omega)Y(x,\omega) \qquad (41)$$

Firstly, let us consider the case of a cylindrical structure, so the matrix A is independent of x.
Waves are obtained by setting $Y(x,\omega) = Z(\omega)e^{px}$ in eq.(41) and thus obtaining the well-known equation providing eigenvalues and eigenmodes

$$(pI - A)Z = 0 \qquad p = p(\omega) \qquad (42)$$

For nondissipative structures, eq.(42) provides, in general n roots for p^2, so the state vector can be written in terms of eigenmodes as

$$Y = Ww \qquad W = [Z_1|Z_2|...|Z_n] \qquad (43)$$

where wave amplitudes satisfy the equation:

$$\frac{dw}{dx} = \Lambda(\omega)w \qquad (44)$$

and $\Lambda(\omega)$ is the diagonal matrix of the eigenvalues.
The propagation function, relating wave amplitudes in two stations is found as

$$X(x_0, x_1, \omega) = diag \ e^{-p_j(x_1-x_0)} \qquad (45)$$

where positive as well as negative values fot the p_j's are to be considered.
Waves amplitudes can be rearranged and partitioned in terms of incoming and outgoing waves, and consequently one obtains the dispersion function $S(\omega)$ given by:

$$S(x_0, x_1, \omega) = \begin{bmatrix} 0 & S_1 \\ S_1 & 0 \end{bmatrix} \qquad (46)$$

where S_1 is the same as X, confined to positive values of p_j's only. For nonuniform structures, special analytical devices should be used [25].

J   Appendix X

Typical electromechanical properties of ceramic piezo-electric materials:

Charachteristic		min value	max value
Piezoelectric Charge	d_{33}	153	593
constant	d_{31}	-60	-274
$(10^{-12}m/V)$	d_{15}	330	741
Elastic constant	Y_{11}^E	6.1	9.3
$(10^{10}N/m^2)$	Y_{33}^E	4.4	7.4

A piezoelectric ceramic can be depolarized by a strong electric field with polarity opposite to the original poling voltage. The limit on the field strength is dependant on the type of material, the duration of the application, and the operating temperature. The typical operating limit is between 500 V/mm and 1000 V/mm for continuous application.

References

[1] Crawley, E.F. and J.de Luis, "Use of Piezoelectric Actuators as Elements of Intelligent Structures", AIAA Journal 2500: 1371-1385, 1987.

[2] Rogers, C.A., "Intelligent Material Systems: The Dawn of a New Materials Age", Journal of Intelligent Materials Systems and Structures, vol.4, no.1, 4-12, 1993.

[3] Wada, B.K., Fanson, J.L. and Crawley, E.F., "Adaptive Structures", The Winter Annual Meeting of the American Society of Mechanical Engineering, 1989.

[4] Davies, G.A.O. and Dorr, D.J., "Aerospace 2020", AGARD S&M Panel, Sesimbra, Portugal, March 1996.

[5] Ikeda, T., "Fundamentals of Piezoelectricity", Oxford University Press, 1990.

[6] Gerhold, C.H. and R. Rocha, "Active Control of Flexural Vibrations in Beam", Journal of Aerospace Engineering 2(3): 141-154, 1989.

[7] Suwei Zhou, Liang, C. and Rogers, C.A., "A Dynamic Model of Piezoelectric Actuator-Driven Thin Plates", in Proceedings SPIE, Smart Structures and Material Conference, Orlando, Florida, 1994.

[8] Sermoneta, A., Liang, C., Sun, F. and Rogers, C.A., "Dynamic Analisys of Active Structures under Multiple Actuators Excitations Using an Impedance Approach", Proceedings SPIE, Smart Structures and Material Conference, San Diego, 1995.

[9] Chandrashekara, K. and Agarwal, A.N., "Active Vibration Control of Laminated Composite Plates Using Piezoelectric Devices: A Finite Element Approach", Journal of Intelligent Material, Systems and Structures, vol.4, 496-508, Oct. 1993.

[10] Santini, P., Battisti, C., Sermoneta, A. and Rotunno, M., "Update Report on ESTEC Contract no. 10.983/94/NL/PP", University of Rome "La Sapienza", Dipartimento Aerospaziale, Feb. 1996.

[11] Balas, M.J., "Direct Velocity Feed-Back Control of Large Space Structures", Journal of Guidance and Control, vol.2, no.3, 252-253, 1978.

[12] Aiako Koike et al., "Torsional and Flexural Control of Sandwich Composite Beams with Induced Strain Actuators", 5th International Conference on Adaptive Structures, Sendai, Japan, 1994.

[13] Santini, P., Betti, F., Gasbarri, P. and Rossi, A., "Actively Damped Piezoelectric Composite Wing", Damping '93, San Francisco, California, Feb. 1993.

[14] Santini, P. et al., "Cantilever Swept Wing of Variable Thickness", L'Aerotecnica. Missili e Spazio, 1986.

[15] Ehlers, S.M. and Weisshaar, T.A., "Static Aeroelastic Behaviour of an Adaptive Laminated Piezoelectric Composite Wing", Proceeding of the 31st AIAA SDM Conference, 1611-1623, Apr.1990.

[16] Ehlers, S.M. and Weisshaar, T.A., "Effect of Adaptive Material Properties on Static Aeroelastic Control", Proceeding of the 33rd AIAA SDM Conference, 914-924, Apr. 1992.

[17] Persiani, F., Gasbarri, P. and Betti, F., "Static Aeroelastic Control of an Adaptive Wing", ICAS Meeting 1994, Anaheim, California, 1994.

[18] Santini, P., Gasbarri, P., Altobelli, M. and Rossi, A., "A Comparative Overview of Strain-Actuated Surfaces Design", 5th International Conference of Adaptive Structures, Sendai, Japan, 1994.

[19] Von Flotow, A.H. and Shafer, B.E., "Wave-Absorbing Controllers for a Flexible Beam", Journal of Guidance, Control and Dynamics, vol.9, no.6, 673-680, 1986.

[20] Von Flotow, A.H. and Pines, D.J., "Active Control of Bending Wave Propagation at Acoustic Frequency", Journal of Sound and Vibration, vol.142, no.3, 391-413, 1990.

[21] Betti, F., "Strutture Adattive nella Tecnologia Aerospaziale", Dissertation Thesis, University of Rome, Dipartimento Aerospaziale, 1993.

[22] Santini, P. and Sermoneta, A., "Structural Analysis of a Multistringer Composite Wingbox", Zeitschrift für Flugwissenshaft und Weltraumforshung, 19(1995), 331-336, Springer Verlag, 1995.

[23] Rossi, A., Liang, C. and Rogers, C.A., "Analysis of Piezoceramic Actuator-Driven System", Center for Intelligent Materials and Structures Report, Virginia Tech, 1992.

[24] Santini, P., "Costruzioni Aeronautiche", editoriale ESA, Roma, 1986.

[25] Santini, P., Battisti, C., Gasbarri, P. and Sermoneta, A., "Wave propagation in Aeronautical Structures", in preparation.

[26] Strelow, H. and Rapp, H., "Smart Materials for Helicopter Rotor Active Control", AGARD Conference Proceedings, Lindau, Germany, 1993.